

ZnO Nanorods on Nanofibrous ZnO Seed Layers by Hydrothermal Method and Their Annealing Effects

K.G. YIM^a, S.M. JEON^b, M.S. KIM^a, S. KIM^c, G. NAM^c, D.-Y. LEE^d, JIN SOO KIM^e,
JONG SU KIM^f AND J.-Y. LEEM^{a,b,*}

^aDepartment of Nano Systems Engineering, Center for Nano Manufacturing, Inje University
Gimhae 621-749, Republic of Korea

^bSMS PE Team 5, MagnaChip Semiconductor Ltd., Gumi 730-723, Republic of Korea

^cSchool of Nano Engineering, Inje University, Gimhae 621-749, Republic of Korea

^dEpi-manufacturing Technology, Samsung LED Co. Ltd., Suwon 443-373, Republic of Korea

^eDivision of Advanced Materials Engineering, Chonbuk National University, Jeonju 561-756, Republic of Korea

^fDepartment of Physics, Yeungnam University, Gyeongsan 712-749, Republic of Korea

ZnO nanorods were grown by using the hydrothermal method on *p*-type Si (100) substrates with nanofibrous ZnO seed layers. Before the ZnO nanorods growth, nanofibrous ZnO seed layers were spin-coated onto the Si substrates. The structural and optical properties of ZnO nanorods were characterized by scanning electron microscopy, X-ray diffraction, and photoluminescence. The fibrous ZnO nanorods is possible due to the surface morphology of the nanofibrous ZnO seed layers. To investigate annealing effects of the ZnO nanorods, the post-annealing process was carried out at various temperatures ranging from 300 to 700 °C under argon conditions. The structural and optical properties of the ZnO nanorods were also affected by the post-annealing treatment.

PACS: 81.05.Dz, 81.15.Lm, 78.55.Et

1. Introduction

ZnO has attracted considerable attention, because it has a hexagonal wurzite structure with a direct wide band-gap of 3.37 eV, a large exciton binding energy of 60 meV at room temperature. These properties of ZnO impose its significant potential in various applications such as in transparent electrodes and blue/UV light emitting diode (LED). Various growth techniques, such as metal-organic chemical vapor deposition (MOCVD) [1], vapor phase transport (VPT) [2], and hydrothermal method [3] have been successful in creating the ZnO nanowires [4], nanorods [2], and nanotubes [5]. Among these growth techniques, hydrothermal method has been studied in view of its simplicity, low growth temperature, large scale growth, flexible application, mass productivity, and the growth of one-dimensional (1D) nanostructure. Recently, 1D nanorods have attracted considerable interest due to their remarkable physical and chemical properties [6]. Several researchers have studied 1D nanorods growth on homogeneous film with various growth conditions [7, 8]. However, there have been few reports considering ZnO nanorods grown on nanofibrous ZnO seed layers by using the hydrothermal method.

In this work, ZnO nanorods on nanofibrous ZnO seed layers were fabricated by using a hydrothermal method. For the post-annealing effects of the ZnO nanorods, they were post-annealed at various temperatures in Ar condi-

tions. The structural and optical properties of the ZnO nanorods were investigated by using field-emission scanning electron microscopy (FE-SEM), X-ray diffraction (XRD), and photoluminescence (PL).

2. Experimental details

The ZnO nanorods were grown by using the hydrothermal method on *p*-type Si (100) substrates with nanofibrous ZnO seed layers. Before the growth of ZnO seed layers, Si substrates were cleaned by immersion in a piranha solution ($\text{H}_2\text{SO}_4 : \text{H}_2\text{O}_2 = 8 : 1$) at 110 °C for 15 min and then in hydrofluoric acid (HF 50% : $\text{H}_2\text{O} = 1 : 9$) for 1 min. Nanofibrous ZnO seed layers were prepared by spin-coating method. The sol solution was prepared by dissolving 0.6 M zinc acetate dehydrate [$\text{Zn}(\text{CH}_3\text{COO})_2 \cdot 2\text{H}_2\text{O}$] in 0.6 M 2-methoxyethanol as a solvent, and monoethanolamine (MEA) was added to the stable sol solution. The molar ratio of MEA to zinc acetate dehydrate was maintained at 1.0. The resultant solution was stirred at 60 °C for 2 h. The sol solution was dropped onto Si substrates, which was rotated at 3000 rpm for 20 s. The ZnO seed layers were pre-heated at 300 °C for 10 min and then cooled in the hot plate (slow cooling). The procedures from spin-coating to pre-heating were repeated three times. The ZnO seed layers were inserted into a furnace and post-heated in air at 450 °C for 1 h. For the synthesis of ZnO nanorods, zinc nitrate hexahydrate [$\text{Zn}(\text{NO}_3)_2 \cdot 6\text{H}_2\text{O}$] and hexamethylenetetramine (HMT) [$\text{C}_6\text{H}_{12}\text{N}_4$] were dissolved in deionized water at room temperature. The concentra-

* corresponding author

tions of both components were fixed at 0.3 M. The substrate was immersed in the aqueous solution. The growth temperature was kept at 140 °C for 6 h. The resultant substrate was rinsed with deionized water and blown dry with nitrogen gas (99.9999%). The ZnO nanorods were annealed at 300, 500, and 700 °C for 20 min under Ar condition by using a thermal annealing system.

3. Results and discussion

Figure 1 shows the SEM image of the ZnO seed layers. The surface of the ZnO seed layers with slow cooling exhibits nanofibrous structure. Zhao et al. [9] reported that the ZnO nanofibrous seed layer was due to the slow cooling. During slow cooling, there is enough time for ions and/or molecules to aggregate along the crystal plane having similar lattice match in order to decrease their high surface energy. This process produces the ZnO nanofibrous nanorods.

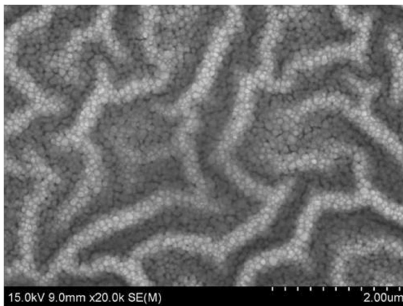


Fig. 1. SEM image of the nanofibrous ZnO seed layers.

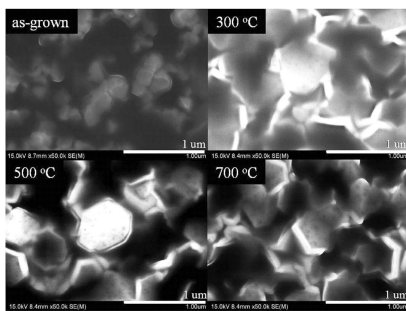


Fig. 2. SEM images of the as-grown ZnO nanorod and ZnO nanorods post-annealed at temperatures of 300, 500, and 700 °C.

Figure 2 shows top-view SEM images of the as-grown ZnO nanorods and the ZnO nanorods at various post-annealing temperature of 300, 500, and 700 °C. The polygonal-shaped ZnO nanorods covered fibrously the Si substrates. The fibrous ZnO nanorods are possible due to the surface morphology of the nanofibrous ZnO seed layers. The formation of ZnO nanorods is influenced by morphology of the seed layers [10]. There are two possible reasons for the formation of the fibrous ZnO nanorods.

One is along the randomly distributed (002) planes of seed layers. As reported by Kim et al. [11], the rugged faceted surface is responsible for the formation of the inclined nanorods due to the preferential formation of the nanorods along the ZnO (002). The density and size of the grown ZnO nanorods depended significantly on the surface morphology and density of ZnO seed layers [12].

As-grown ZnO nanorods were post-annealed at 300, 500, and 700 °C in Ar condition. After post-annealing, the nanopores of ≈ 50 nm are observed at the surface of ZnO nanorods and the diameters of the ZnO nanorods are increased from 200 to 500 nm. For high annealing temperature, the nanopore size increases gradually. According to forming the nanofibrous seed layer by slow cooling, the ZnO nanorods were inclined.

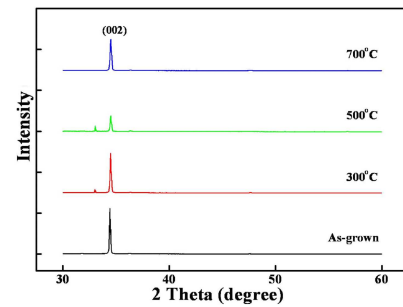


Fig. 3. XRD diffraction patterns of the as-grown ZnO nanorod and ZnO nanorods post-annealed at temperatures of 300, 500, and 700 °C.

Figure 3 shows the XRD patterns of the as-grown ZnO nanorods and annealed ZnO nanorods. For all the samples, the diffraction peaks of (002) are only observed. The (002) diffraction peak located at 34.5° is the most intensive. In generally, the ZnO (002) peak indicate that the preferred orientation due to the lowest surface energy is along the (001) basal plane in ZnO [13].

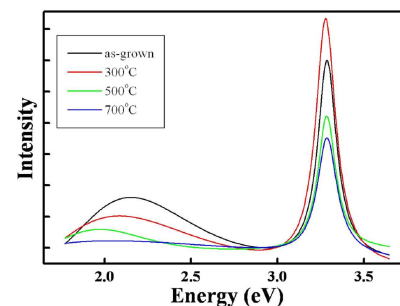


Fig. 4. PL spectra of the as-grown ZnO nanorod and ZnO nanorods post-annealed at temperatures of 300, 500, and 700 °C.

Figure 4 PL measurements were carried out at room temperature to examine the effect of the post-annealing on the optical properties of the ZnO nanorods. Figure 4 shows the PL spectra of the as-grown ZnO nanorods and

the annealed ZnO nanorods. All of the samples exhibit two emission peaks. One is the strong UV region and the other is the weak deep-level emission (DLE) at visible region. The UV emission is the exciton recombination related near-band edge emission (NBE) and the DLE usually accompanies the presence of structural defects and impurities [14]; these can include an oxygen vacancy (V_O), a zinc vacancy (V_{Zn}), an oxygen atom at the zinc position in the crystal lattice (O_{Zn}), a zinc atom at the oxygen position in the crystal lattice (Zn_O), interstitial oxygen (O_i), and interstitial zinc (Zn_i). The NBE peak position is around 3.285 eV, and the NBE peak position is hardly affected by the existence of pores at the surfaces of the ZnO nanorods. However, the DLE peak is shifted from green-yellow to orange region as pores are formed on the surfaces of the ZnO nanorods. Besides, the DLE peak is red-shifted from orange to red region with the post annealing temperature increase of the ZnO nanorods. The green-yellow emission (500–600 nm) and orange (610 nm) in ZnO has been attributed to intrinsic defects such as Zn_i and V_O [15] and interstitial defects such as O_i [16]. Few studies have reported red emissions in undoped ZnO, and the origin is still under debate.

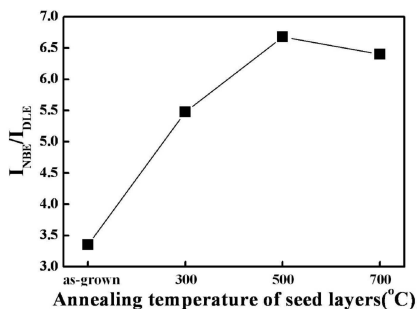


Fig. 5. PL intensity ratio of the NBE to the DLE as a function of the post-annealing temperatures.

Figure 5 shows the PL intensity ratio of the NBE to the DLE as a function of the post-annealing temperature. In general, the large intensity ratio of the NBE to the DLE indicates that the ZnO nanorods have better optical properties. It can be seen that intensity ratio of the NBE to the DLE increases in post-annealed ZnO nanorods compared to the as-grown ZnO nanorods. The PL intensity ratio of the samples increased from 3.35 to 6.68 as the post-annealing temperature increased. The bigger the intensity ratio, the higher the quality of the ZnO nanorods [17]. Improved emission efficiency has also been reported in porous GaN [18]. The improvement of the post-annealed ZnO nanorods is explained in terms of increase of the emission rate of excess carriers due to the porous ZnO nanorods.

4. Conclusions

The ZnO nanorods on nanofibrous seed layers were grown by using hydrothermal method and were post-annealed in Ar condition at temperature of 300, 500,

and 700°C for 20 min. The formation of as-grown ZnO nanorods is influenced by morphology of the nanofibrous ZnO seed layers. After post-annealing, the nanosized pores are formed on the surfaces of ZnO nanorods. As the post-annealing temperature increased, the PL intensity ratio significantly increased. Post-annealing process of ZnO nanorods plays an important role in enhancing the optical properties.

Acknowledgments

This research was supported by Basic Science Research Program through the National Research Foundation of Korea (NRF) funded by the Ministry of Education, Science and Technology (No. 2011-0003067).

References

- [1] W.I. Park, D.H. Kim, S.-W. Jung, G.-C. Yi, *Appl. Phys. Lett.* **80**, 4232 (2002).
- [2] S. Oh, M. Jung, J. Koo, Y. Cho, S. Choi, S. Yi, G. Kil, J. Chang, *Physica E* **42**, 2285 (2010).
- [3] B. Liu, H.C. Zeng, *J. Am. Chem. Soc.* **125**, 4430 (2003).
- [4] Y. Li, G.W. Meng, L.D. Zhang, *Appl. Phys. Lett.* **76**, 2011 (2000).
- [5] Y.-J. Xing, Z.H. Xi, Z.Q. Xue, X.D. Zhang, J.H. Song, *Appl. Phys. Lett.* **83**, 1689 (2003).
- [6] J. Wang, M.S. Gudiksen, X. Duan, Y. Cui, C.M. Lieber, *Science* **293**, 1455 (2001).
- [7] J.-J. Wu, S.-C. Liu, *J. Phys. Chem. B* **106**, 9546 (2002).
- [8] S.-H. Park, S.-Y. Seo, S.-H. Kim, *Appl. Phys. Lett.* **88**, 251903 (2006).
- [9] J. Zhao, Z.-G. Jin, T. Li, X.-X. Liu, *J. Eur. Ceram. Soc.* **26**, 2796 (2006).
- [10] B.H. Kong, H.K. Cho, *J. Cryst. Growth* **289**, 370 (2006).
- [11] D.C. Kim, B.H. Kong, H.K. Cho, D.J. Park, J.Y. Lee, *Nanotechnology* **18**, 015603 (2007).
- [12] S.-D. Lee, Y.-S. Kim, M.-S. Yi, J.-Y. Choi, S.-W. Kim, *J. Phys. Chem. C* **113**, 8954 (2009).
- [13] M.S. Kim, K.G. Yim, M.Y. Cho, J.-Y. Leem, D.-Y. Lee, J.S. Kim, J.S. Kim, J.-S. Son, *J. Korean Phys. Soc.* **58**, 515 (2011).
- [14] S.-H. Jeong, B.-S. Kim, B.-T. Lee, *Appl. Phys. Lett.* **82**, 2625 (2003).
- [15] Y.-Y. Peng, T.-E. Hsieh, C.-H. Hsu, *Nanotechnology* **17**, 174 (2006).
- [16] S.A. Studenikin, N. Golego, M. Cocivera, *J. Appl. Phys.* **84**, 2287 (1998).
- [17] S.W. Xue, X.T. Zu, W.G. Zheng, M.Y. Chen, X. Xing, *Physica B* **382**, 201 (2006).
- [18] A.P. Vajpeyi, S. Tripathy, S.J. Chua, E.A. Fitzgerald, *Physica E* **28**, 141 (2005).